Synthetic Metals 267 (2020) 116462

Contents lists available at ScienceDirect

Synthetic Metals

journal homepage: www.elsevier.com/locate/synmet

Effects of small-molecule-doping on spin-assisted processes in P3DDT:$PC_{61}BM$ photovoltaics

V.I. Krinichnyi*, E.I. Yudanova, N.N. Denisov, V.R. Bogatyrenko

Department of Kinetics and Catalysis, Institute of Problems of Chemical Physics RAS, Academician Semenov Avenue 1, Chernogolovka, 142432, Russia

ARTICLE INFO

Keywords:
Charge recombination
Light-induced electron paramagnetic resonance
Organic photovoltaics
Spin dynamics
Spin relaxation

ABSTRACT

The influence of the 1,2-benzopyrone (BP) and 2,5-diphenyloxazole (PPO, DPO) additives on the formation, separation, motion and recombination of charge carriers in the poly(3-dodecylthiophene):[6,6]-phenyl-C_{61}-butanoic acid methyl ester (P3DDT:$PC_{61}BM$) organic photovoltaics was investigated by the light-induced electron paramagnetic resonance (LEPR) and NIR-Vis-UV spectroscopy within the wide temperature and photon energy range. These processes were interpreted in the framework of the exchange interaction of spin ensembles differently distributed in bulk heterojunctions of the P3DDT:$PC_{61}BM$ composite. The concentration, composition and dynamics of spin charge carriers were shown to be determined by the modification degree of the sample with small molecules, the energy of the light photons as well as the number, spatial distribution and energetic depth of spin traps formed in the disordered polymer matrix. Electronic functionality of the composite becomes better after its doping with BP and PPO additives up to optimal weight levels of 0.03 and 0.06, respectively. Such modification can improve the morphology/ordering of the composite that increases the number of highly mobile charge carriers due to the release of a part of carriers captured by energetically deep spin traps. This increases an exchange interaction between spin ensembles, reduces the number and depth of electron spin traps that, in turn, prevents the recombination of charge carriers and accelerates the power conversion.

1. Introduction

Organic polymer semiconductors with unique electronic properties have attracted great attention due to the prospects of their use as active matrices of various molecular devices, e.g, field effect transistors, photodiodes, sensors, and solar cells [1]. Such devices are characterized by simple manufacturing, low cost with, however, high functionality and efficiency. Solar cells normally consist of π-conjugated polymer/copolymer and fullerene derivatives which act as electron donating and accepting groups, respectively, and convert solar illumination into electrical energy with the efficiency of 10–17 % [1–3]. Light photons generate in bulk heterojunctions (BHJ) of such solar cells coupled singlet excitons, the subsequent dissociation of which leads to the formation of positively charged polaron on the polymer chain and negatively charged fullerene radical anion between the polymer chains [2]. This light conversion process consists of several elemental stages: i) exciton generation upon absorption of light photon; ii) exciton diffusion to the boundary of the donor and acceptor phases in BHJ; iii) formation of a coupled electron-hole pair at the interface of these phases, and its subsequent dissociation into a pair of free charge carriers; and, finally, iv) transport of charge carriers in the direction of the corresponding electrodes. At each of these stages, bimolecular geminal or monomolecular non-geminal recombination of charge carriers can occur, depending on the structural and morphological properties of a composite. Optimizing the morphology can shift the balance of initiation and recombination of spin charge carriers, and thus increase the efficiency of solar energy conversion.

A fundamental problem of real organic photovoltaic (OPV) elements is the formation in their BHJ of energetically deep spin traps due to the disordering of their backbones. Because both charge carriers formed from initial excitons possess spin $S = ½$, such traps capture the corresponding charge carriers till they are fully filled and decrease the effective rate of spin transport. Immobilized carriers can be detrapped to the free state due to their interaction with lattice phonons [4]. Then they can either be trapped by vacant trap sites or recombine with trapped counter charges. Earlier it was showed [5] a significant influence of the number, depth and spatial distribution of spin traps on electronic properties of various polymer:fullerene composites.

Interaction of spin charge carriers with other spin ensembles and own magnetic or/and dipole microenvironment also plays a key role in the charge transport in OPV systems. Various factors can influence the intrinsic magnetic resonance properties of spins in organic solids, the

* Corresponding author.
E-mail address: kivi@cat.icp.ac.ru (V.I. Krinichnyi).

https://doi.org/10.1016/j.synthmet.2020.116462
Received 1 April 2020; Received in revised form 1 June 2020; Accepted 3 June 2020

strongest of which are their magnetic dipole–dipole and Heisenberg exchange interactions [6]. Because both the charge carriers photoinitiated in a polymer:fullerene system exchangeable spin-flip, this process becomes dependent on their concentration, dynamics, polarization and mutual separation. In some cases, exchange interaction may convert the state of spin pairs from singlet to triplet [7]. The lifetime of triplet pairs is longer than singlet one, so then such species have a better chance to dissociate in BHJ. So, spin interaction accelerates the recombination of the resulting charge carriers, originating a balance of the excited and recombined spin pairs. This should affect the electronic properties of the respective composite and thus the efficiency of its conversion of the light energy. The knowledge of structure and properties of composite is required to improve its electronic properties. So, the efficiency and functionality of such systems should be determined by their structure and morphology which governs spin-assisted separation, coupling and recombination of free charge carriers formed in their BHJ. However, the relationship between structural and spin properties of these compounds still remains unknown.

It was pointed out that the adding of small molecules, e.g., pyrrole derivatives [8,9] or di-iodooctane [10], into polymer OPV systems improves the mixing and packing of its components at the molecular level, reduces the number of electron traps and optimizes its morphology. This prolongs separation of the charges, accelerates their dynamics, suppress their recombination and thereby improve their efficiency of the energy conversion. On the other hand, such improvement can be reached by the flipping interaction of spin charge carriers with paramagnetic adduct, e.g., radical galvinoxyl [7], introduced as dopant into a polymer:fullerene system. In this case, the recombination of spin pairs should be suppressed by resonant exchange interaction between such spin adducts and charged acceptors, which converts the singlet state of spin pairs to triplet one. Therefore, neither clear explanation of the influence of molecular additives on the system structural and morphological properties nor the correlation of these parameters with the properties of spin charge carriers has been obtained.

1,2-Benzopyrone (BP, coumarin), 2,5-diphenyloxazole (PPO, DPO) and their derivatives are relatively cheap and easy to synthesize stable dispersants, anticoagulants, converters of electron energy excitation can also be considered as prospected materials for appropriated molecular devices. This stimulated their extensive study and creation of nonlinear optical elements, lasers, scintillators, fluorescent probes, sensors, other electronic and photonic devices with respective functional matrices [11]. Undoubtedly, these additives should also provoke the improving of molecular and electronic properties of molecular elements in which the charges are transferred by spin carriers.

Despite the widely using of organic nanomaterials as active matrix in molecular devices, however, surprisingly little is known about the exact roles that different experimental parameters have in tuning their final functionality and electronic properties. It is hereby of crucial importance to understand the connection between these properties and their lowed-dimensional structure, morphology and composition.

For the study of OPV systems can be used various methods, including femtosecond time-resolved optically- and absorption-detected magnetic resonance methods [12]. However, these indirect methods able only determine an effective number of different carriers formed from excitons. Spin nature of these carriers plays a crucial role in the main properties of organic devices. Because both charge carriers possess spin $S = ½$. the processes carrying out in such systems can be study more accurately by continuous wave (cw) and pulse magnetic resonance methods. However, the latter often provide ambiguous results concerning spin coupling, relaxation and dynamics in some spin-labeled [13] and π-conjugated polymer systems [14–16], including OPV composites [17]. This is why the direct cw electron paramagnetic resonance (cw EPR) spectroscopy is widely used for detailed investigation of spin-assisted processes in various organic polymer systems [15,16,18,19]. Multifrequency cw EPR method was used to analyze the magnate, relaxation and dynamics properties of spin charge carriers stabilized in a variety of an initial and doped π-conjugated polymers [20]. Light-Induced cw EPR (cw LEPR) spectroscopy was used for the study of charge photoexcitation, separation, transfer, and recombination in various polymer:fullerene composites [2,[5],21]. It was found that the *g*-factors of both charge carriers photoinitiated in these systems are close to the *g*-factor of the free electron, $g_e = 2.00232$. This causes partial or complete overlapping of their contributions to the effective cw LEPR spectra. Therefore, for a more accurate determination of the main magnetic resonance parameters of all spin ensembles (concentration, linewidth, *g*-factor, etc.) and analysis of their change upon experimental conditions, the deconvolution of the cw LEPR spectra should be made [5a,18,22,23]. This allows us to determine the main magnetic resonance parameters separately for all mobile and captured spin charge carriers and control them upon variation of environmental parameters. Such procedure allowed also to estimate the composition, spatial distribution, local concentration of spin charge carriers photoinitiated in different OPV composites [5a]. It was shown that BHJ formed by the chains of regioregular poly(3-dodecylthiophene) (P3DDT) with the fullerene derivative [6,6]-phenyl-C_{61}-butanoic acid methyl ester ($PC_{61}BM$) are the most convenient model system for studying spin-assisted properties of respective photovoltaic systems. The extended alkyl substituents of P3DDT act as insulating envelopes of its π-conjugated chains, so then preventing an interaction of far separated spins situated on the adjacent chains.

In the present work, we report the first results of a detailed comparative cw LEPR study of spin-assisted photoexcitation, relaxation, dynamics, and recombination of charge carriers photoinitiated in the P3DDT:$PC_{61}BM$ BHJ doped with the BP and PPO molecules using variable photoexcitation energy at wide temperature range in combination with spectral simulations. The data obtained allowed us to determine the correlations of the main parameters of photoinitiated spin charge carriers with the structure, composition of the initial and differently doped BHJ. This made it possible to conclude the key role of small molecules in structuring the polymer:fullerene BHJ, which increases the stability of spin charge carriers and energy-converting functionality.

2. Experimental details

2.1. Ingredients used in experiments

In the work, regioregular P3DDT with the HOMO = −5.29 eV, LUMO = −3.55 eV [24] and lattice constants of $a = 2.583$ nm, $b = 0.775$ nm, and $c = 0.777$ nm [25] distributed by the Aldrich (USA), [6,6]-phenyl-C_{61}-butanoic acid methyl ester ($PC_{61}BM$) with the HOMO = -6.10 eV, LUMO = −3.75 eV [26] distributed by the Solenne BV (The Netherlands), were used without additional rectification as electron donating and accepting groups, respectively. 1,2-Benzopyrone, $C_9H_6O_2$ (BP, coumarin) with the bandgap of $E_g = 3.99$ eV [27], 2,5-diphenyloxazole, $C_{15}H_{11}NO$ (PPO, DPO) with the bandgap of $E_g = 3.79$ eV [28], distributed by the Aldrich® (USA) were used for the doping of the P3DDT:$PC_{61}BM$ BHJ. The chemical structures of these components are shown schematically in Fig. 1.

2.2. Preparation of the samples

In order to prepare the P3DDT:$PC_{61}BM$ composite with a 1:1 wt. ingredient ratio, first 6 mg of P3DDT and 6 mg of $PC_{61}BM$ were solved in 1.1 mL of dichlorobenzene. This solution was treated in ultrasonic cleaner DADI DA-968 (50 W) for 10 min with the following warming at $T = 333$ K for 10 min and further ultrasonic treatment within 10 min. Then 2.6 mg of the BP additive was additionally solved in 1 mL dichlorobenzene and added to the above P3DDT:$PC_{61}BM$ chlorobenzene solution at 3 %, 6 %, 9 %, and 21 % by weight and the respective P3DDT:$PC_{61}BM$ solutions were each casted 7 times by 5 μL into both sites of a separate ceramic plate with subsequent drying in air until they

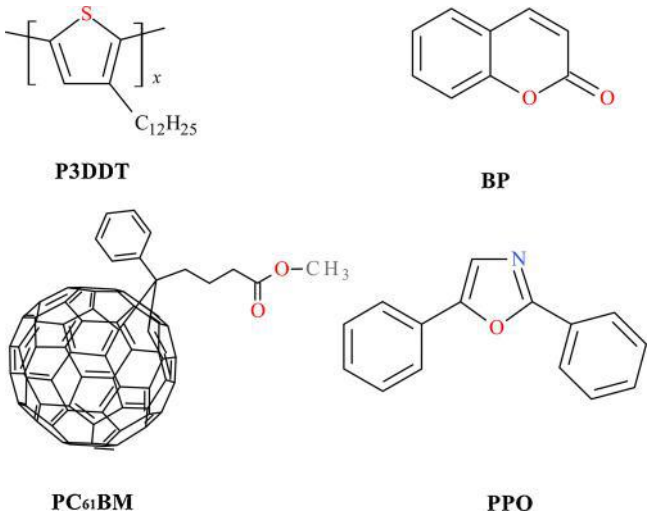

Fig. 1. Chemical structures of poly(3-dodecylthiophene) (P3DDT), [6,6]-phenyl-C_{61}-butanoic acid methyl ester ($PC_{61}BM$), 1,2-benzopyrone, coumarin (BP), and 2,5-diphenyloxazole (PPO) used in this study.

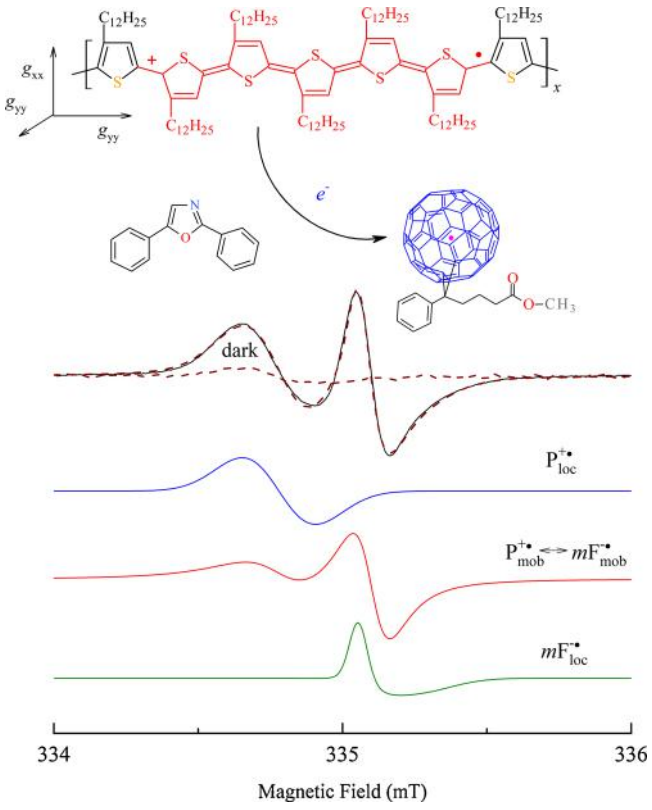

Fig. 2. X-band (9.5 GHz, 334 m T) LEPR spectra of charge carriers background initiated in the P3DDT:$PC_{61}BM$/$PPO_{0.06}$ BHJ at T = 77 K by chromatic light with the photon energy of $h\nu_{ph}$ = 1.88 eV. Lorentzian LEPR spectrum best fitting the effective experimental LEPR one with contributions caused by polarons and methanofullerene radical anions immobilized in a polymer matrix, $P^{+\bullet}_{loc}$ and $mF^{-\bullet}_{loc}$, respectively, as well as by highly mobilized radical pairs, $P^{+\bullet}_{mob} \leftrightarrow mF^{-\bullet}_{mob}$ with g^{P}_{iso} = 2.00182, g^{mF}_{iso} = 1.99983, ΔB^{P}_{pp} = 0.158 m T, ΔB^{mF}_{pp} = 0.110 m T and relative concentrations n^{P}_{loc}: n^{P}_{mob}: n^{mF}_{mob}: n^{mF}_{loc} = 2.20:2.28:2.28:1.00 are shown as well. In the top are schematically shown the structural BHJ formed in the polymer nanocomposite. The transfer of an elementary negative charge from polymer chain to methanofullerene molecule accompanied by the formation on the former of polaron $P^{+\bullet}$ (hole) with an elementary positive charge and spin S = ½ is shown as well. The orientation of the principal axes of the polaron's ***g***-tensor is also given.

were formed as double-sided films, both with the size of ca. 4 × 8 mm^2 and thickness of ca. 0.1 mm. As a result of this procedure, except of the initial donor-accepter P3DDT:$PC_{61}BM$ composite (shown in the top of Fig. 2), the samples with the weight doping level of y = 0.03, 0.06, 0.09, and 0.21 were obtained.

2.3. NIR-Vis-UV absorption spectra of polymer composites

Optical absorption spectra of the samples were obtained by using spectrophotometer Specord-250 plus (Analytik Jena) at their scanning within the band 1.13–6.53 eV (1100 − 190 nm) at T = 298 K. Low-energetic 1.24–3.6 eV (1000 − 344 nm) spectral regions of the P3DDT matrix as well as the initial and optimally doped P3DDT:$PC_{61}BM$ composites are shown in Fig. 3a. The composition and positions of the spectral components were determined accurately by using the differentiation of experimental absorption spectra.

2.4. Photoinitiation of spin charge carriers

The samples situated in the center of the MW cavity of the EPR spectrometer were illuminated trough the quartz cylindrical light guide by the 5 − 10 W Luxeon LED monochromatic sources with the photon energy $h\nu_{ph}$/wavelength λ_{ph}/luminous emittance I_l of 1.34 eV/923 nm/354 lx, 1.49 eV/834 nm/500 lx, 1.75 eV/707 nm/963 lx, 1.90 eV/653 nm/4870 lx, 1.99 eV/622 nm/1930 lx, 2.11 eV/587 nm/762 lx, 2.38 eV/522 nm/1026 lx, 2.49 eV/497 nm/1180 lx, 2.82 eV/439 nm/2740 lx, 2.76 eV/450 nm/7430 lx, 3.02 eV/411 nm/1660 lx, 3.15 eV/394 nm/1450 lx, 3.29 eV/377 nm/1750 lx, and 3.40 eV/365 nm/2070 lx, as well as achromatic, white sources with the correlated color temperature (CCT) of T_c = 15000, 5500, 3700, and 3300 K and luminous emittance I_l = 2620, 4960, 4020, and 3220 lx, respectively. The light of was passed to the spectrometer through a quartz fiber accurately reproducing a similar process at the EPR MW cavity. The radiation spectra of these LED sources were previously measured by the spectrometer FSD-9 ("Optofiber") equipped with a 16-bit analog-to-digital converter and connected to a computer with respective software. The I_l values of the sources were determined using the IMO-2 N broadband bolometric light emission power meter and LX-1010BS digital luxmeter and were used for further normalization of the number of spins photoinitiated in the composites under study.

2.5. LEPR spectra measurements and processing

CW EPR measurements were performed using PS-100.X spectrometer operating at 3-cm waveband (9.7 GHz) with a 150 mW maximal MW power and 100 kHz synchronous detection. Dark and photoinduced LEPR spectra of the initial and doped P3DDT:$PC_{61}BM$ nanocomposites were obtained at 77 K being inserted into a quartz Dewar filled with liquid nitrogen and placed into a center of the MW cavity of EPR spectrometer. For EPR measurements at temperature range of T = 90–320 K, the samples were situated in a quartz flow Dewar cell and centered in a stream of dry nitrogen, whose temperature was stabilized by the BRT SKB IOC controller, equipped with a platinum temperature sensor pt100. The signal-to-noise ratio of registering signals was improved by their accumulation during their multiple field scanning. The processing and simulation of the spectra were performed using the EasySpin [29] and OriginLab programs. Spectral contribution and concentration of spin charge carriers were determined separately by decomposing of effective EPR spectra registered far from their MW saturation combined with the "light on-light off" procedure described earlier [5a,30]. Landé g-factors of spin charge carriers were determined using the *N,N*-diphenyl-N'-picrylhydrazyl (DPPH) standard with g = 2.0036 ± 0.0002 [31]. The accuracy of estimating the intensity I, g-factor of the line and the distance between its positive and negative spectral peaks ΔB_{pp} was determined to be 5%, ± 2 × 10^{-4} and ± 2 × 10^{-3} mT, respectively. The times of spin-lattice T_1 and spin-spin T_2

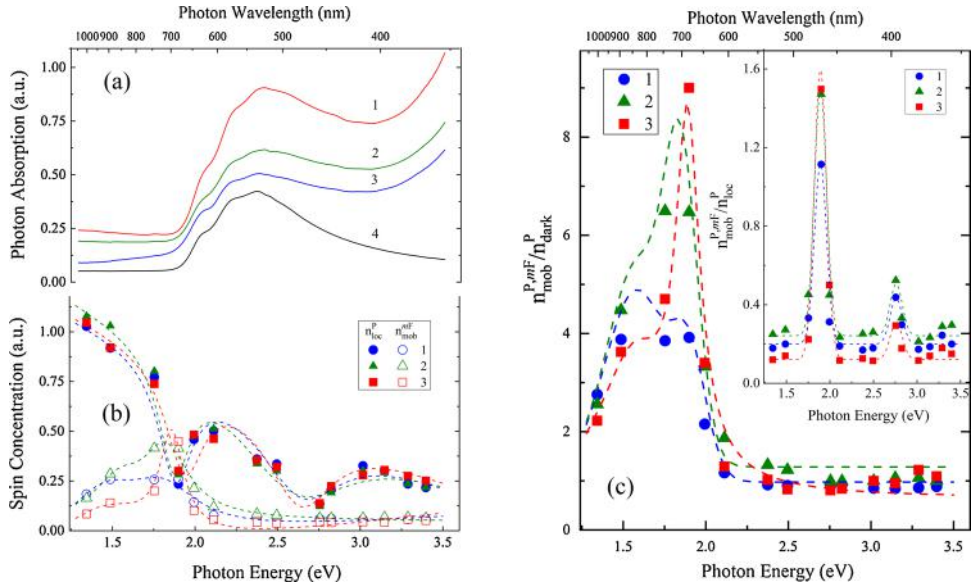

Fig. 3. (a) The NIR-Vis-UV absorption spectra of the initial P3DDT backbone (4), its composites P3DDT: $PC_{61}BM$ (3), P3DDT:$PC_{61}BM/BP_{0.03}$ (2) and P3DDT: $PC_{61}BM/PPO_{0.06}$ (1) obtained at $T = 298$ K. (b) Spin concentrations of the captured polarons $P^{+\bullet}_{loc}$ (filled points) and mobile methanofullerene radical anions $mF^{-\bullet}_{mob}$ (open points) photoinitiated in the initial P3DDT: $PC_{61}BM$ BHJ (1) as well as in the optimally modified P3DDT: $PC_{61}BM/BP_{0.03}$ (2) and P3DDT:$PC_{61}BM/PPO_{0.06}$ (3) samples as function of the energy of initiating photons $h\nu_{ph}$. (c) The $n^{P,mF}_{mob}/n^{P}_{dark}$ and $n^{P,mF}_{mob}/n^{P}_{loc}$ (insert) rations determined for the mobile and captured polarons $P^{+\bullet}$, as well as for methanofullerene anion radicals $mF^{-\bullet}$ photoinitiated in the initial P3DDT: $PC_{61}BM$ BHJ (1) as well as in the P3DDT:$PC_{61}BM/BP_{0.03}$ (2) and P3DDT: $PC_{61}BM/PPO_{0.06}$ (3) samples as function of the energy of initiating photons $h\nu_{ph}$. The dashed lines are drawn arbitrarily only for illustration to guide the eye.

relaxation of spin ensembles were determined upon their steady-state MW saturation regime according the method earlier described [32].

3. Results and discussion

3.1. Spin composition and magnetic resonance parameters

The darkened initial and modified P3DDT: $PC_{61}BM$ composites demonstrate typical weak EPR spectra shown in Fig. 2. The observed spins can be attributed to charge carriers excited by infrared phonons irradiated by active internal elements of the EPR spectrometer and captured by energetically deep spin traps formed in the polymer backbone due to its disordering. No features of radical species involving BP and PPO were observed. Once the samples are illuminated by the light photons, paramagnetic polarons, $P^{+\bullet}$, and methanofullerene radical anions, $mF^{-\bullet}$, are photoinitiated in their internal BHJ. The first photoinitiated carriers fill the remaining above-mentioned spin traps and become localized, whereas the subsequent carriers transfer the charge along and between polymer chains. Besides, polarons initiated on adjacent polymer chains can merge into mobile diamagnetic $P^{+\bullet}_{mob} \leftrightarrow P^{+\bullet}_{mob}$ or immobilized paramagnetic $P^{-\bullet}_{loc} \leftrightarrow P^{+\bullet}_{loc}$ bipolarons with equal g-factors [33], the double arrows mean the formation of such polaron pairs. The balance polaron ↔ bipolaron can also to change the experimental LEPR spectra. Fig. 2 exhibits an exemplar effective X-band (9.5 GHz, 334 m T) LEPR spectrum of charge carriers background initiated in the P3DDT:$PC_{61}BM/PPO_{0.06}$ BHJ at $T = 77$ K by monochromatic light source with the photon energy of $h\nu_{ph} = 1.88$ eV. In order to separate the contributions of the free and captured charge carriers into the sum LEPR spectra and to control their changes at different experimental conditions, they should be deconvoluted according the procedure described earlier [23,34]. Lorentzian LEPR spectrum best fitting the effective experimental LEPR one with own contributions caused by polarons and methanofullerene radical anions immobilized in a polymer matrix, $P^{+\bullet}_{loc}$and $mF^{-\bullet}_{loc}$, respectively, as well as by highly mobilized radical pairs $P^{+\bullet}_{mob} \leftrightarrow mF^{-\bullet}_{mob}$, with $g^{P}_{iso} = 2.00182$, $g^{mF}_{iso} = 1.99983$, $\Delta B^{P}_{pp} = 0.158$ m T, $\Delta B^{mF}_{pp} = 0.110$ m T and relative concentrations n^{P}_{loc}: n^{P}_{mob}: n^{mF}_{mob}: $n^{mF}_{loc} = 2.20{:}2.28{:}2.28{:}1.00$ are also shown in the Fig. 2. The structures of BHJ formed in the polymer nanocomposite are schematically shown in the top of the Figure as well. The values of magnetic resonance parameters obtained lie near those determined for the other thiophene-based composites [23,34]. An analysis of LEPR spectra showed their dependence on modification of the sample by both the BP and PPO small molecules. Concentration, relaxation and dynamic parameters of both spin charge carriers photoinduced in the P3DDT:$PC_{61}BM$ BHJ with different, e.g., BP content are presented in Table 1. These parameters were analyzed to change strongly as the sample is doped with the BP and PPO up to $y = 0.03$ and 0.06, respectively (see below). In order to achieve the better simplicity and clarity, in the next paragraphs are discussed mainly the comparative results obtained in the study of the initial, P3DDT:$PC_{61}BM$, P3DDT:$PC_{61}BM/BP_{0.03}$ and P3DDT:$PC_{61}BM/PPO_{0.06}$ composites.

3.2. Optics and paramagnetic absorption

Fig. 3a shows effective spectra of the initial P3DDT matrix, P3DDT:$PC_{61}BM$ composite as well as the exemplar composites P3DDT:$PC_{61}BM/PPO_{0.06}$ and P3DDT:$PC_{61}BM/BP_{0.03}$. These spectra are a superposition of spectral contributions of respective ingredients and contain the bands registered in the UV and Vis regions of the sum spectra. Their UV spectral contributions (not shown in the Figure) are characterized by a set of peaks registered at 3.69, 4.66 and 5.74 eV (336, 266 and 216 nm), which can be attributed to the C_{60} fragment of methanofullerene $PC_{61}BM$ [35]. The BP adduct brings into UV region an additional bands lying near 3.88 and 4.43 eV (320 and 280 nm) [36]. On the other hand, the PPO band contribution without pronounced spectral extremes lies in the 3.91–4.09 eV (317 to 303 nm) absorption region [37]. Its Vis-peak situated near 2.38 eV (522 nm) was attributed to the HOMO π – LUMO π* transition of the P3DDT backbone [38]. These values correlate with the energy of the π–π* interband transition, that should to indicate a pronounced planarity of the chains of P3DDT backbone. This is due to a decrease in the number of possible conformations of the polymer chains with the side lengthy alkyl substitutes, which prevents rotating of thiophene units around C—C bonds [39]. The weak broad absorption contribution with maxima of about 2.06 and 2.20 eV (602 and 564 nm) observed in the region 1.85–2.82 eV (670 – 440 nm) can be attributed to the forbidden first order transitions

Table 1
The concentration ratio n_{mob}^{mF}/n_{loc}^{P}, linewidth ΔB_{pp}^{P} ad B_{pp}^{mF}, spin relaxation times T_1^P, T_2^P and T_1^{mF}, T_2^{mF}, diffusion coefficients D_{1D}^{P}, D_{3D}^{P} and D_{lb}^{mF} determined for polarons $P^{+\bullet}$ and methanofullerene radical anions $mF^{-\bullet}$ excited in the P3DDT: $PC_{61}BM/BP_y$ BHJ with different BP-doping weight level *y* upon illumination by photons with the energy (wavelength) of $h\nu_{ph}$ = 1.88 eV (λ_{ph} = 660 nm) and *T* = 77 K.

y Parameter	0.00	0.03	0.06	0.09	0.21
n_{loc}^{P}/dark	2.874	3.596	3.330	3.451	2.588
n_{mob}^{mF}/n_{loc}^{P}	1.115	1.471	1.503	0.786	1.065
ΔB_{pp}^{P}, mT	0.156	0.159	0.158	0.162	0.140
ΔB_{pp}^{mF}, mT	0.107	0.110	0.110	0.109	0.102
T_1^P, s	6.1×10^{-7}	3.6×10^{-7}	1.4×10^{-7}	3.4×10^{-7}	1.9×10^{-7}
T_2^P, s	4.2×10^{-8}	4.2×10^{-8}	4.16×10^{-8}	4.1×10^{-8}	4.4×10^{-8}
T_1^{mF}, s	5.9×10^{-7}	6.5×10^{-7}	4.0×10^{-7}	8.1×10^{-7}	4.5×10^{-7}
T_2^{mF}, s	6.2×10^{-8}	6.0×10^{-8}	5.9×10^{-8}	6.0×10^{-8}	6.0×10^{-8}
D_{1D}^{P}, rad/s	1.37×10^{12}	9.56×10^{11}	5.55×10^{10}	3.31×10^{11}	1.14×10^{11}
D_{3D}^{P}, rad/s	4.21×10^{5}	5.42×10^{5}	1.45×10^{7}	1.68×10^{6}	7.59×10^{6}
D_{lb}^{mF}, rad/s	6.72×10^{10}	6.43×10^{10}	1.01×10^{11}	4.98×10^{10}	8.99×10^{10}

in the C_{60} fragment of methanofullerene [40].

Fig. 3b shows how changes the number of polarons $P_{loc}^{+\bullet}$ and pairs of highly mobile charge carriers, $P_{mob}^{+\bullet} \leftrightarrow mF_{mob}^{-\bullet}$, photoinitiated and recombined in the exemplary P3DDT:$PC_{61}BM/PPO_{0.06}$ BHJ. Previously, it was shown [5a] that the number and composition of such paramagnetic centers photoinitiated in organic polymer:fullerene composites are determined by their structure, morphology as well as by the energy of the initiating light photons and temperature. Similar peculiarities are expected also for the composites under study. However, the comparison of the data presented in Fig. 3a and b evidence that the number of photons absorbed by the samples does not correlates with the number of resulting spin charge carriers. One can note only a close change of the number of localized polarons and absorbed photons within the energy range $h\nu_{ph}$ = 2.0–2.5 eV. Such discrepancy can be due to the above mentioned formation of localized bipolarons with equal *g*-factors in adjacent polymer chains [33]. The control of these parameters should to be simpler if one analyzes the ratio of the concentrations of mobile charge carriers to the immobilized paramagnetic centers. Indeed, the data presented in Table 1 evidences that the higher concentration ratio of mobile methanofullerene radical anions (and polarons) to that of localized polarons, $n_{mob}^{mF}/n_{loc}^{P} \equiv n_{mob}^{P}/n_{loc}^{P}$, excited in the P3DDT:$PC_{61}BM/PPO_{0.06}$ BHJ the easier and faster the charges are transferred between the chains and, therefore, the better efficiency of energy conversion should be realized for the respective photovoltaic system.

Fig. 3c depicts the $n_{mob}^{P,mF}/n_{dark}^{P}$ and $n_{mob}^{P,mF}/n_{loc}^{P}$ (in the insert) rations determined for the mobile and captured polarons $P^{+\bullet}$, as well as of methanofullerene radical anions $mF^{-\bullet}$ photoinitiated in the initial P3DDT:$PC_{61}BM$ BHJ as well as in the P3DDT:$PC_{61}BM/PPO_{0.06}$ and P3DDT:$PC_{61}BM/DA_{0.03}$ samples as function of the energy of initiating photons $h\nu_{ph}$. It is seen from the Figure that the addition of a certain number of molecules PPO or BP to the initial composite causes a significant increase in the number of both mobile charge carriers, which is accompanied by a corresponding decrease in these carriers excited by lower-energy photons. The other main feature of the data presented is a significant decrease of the ratio $n_{mob}^{P,mF}/n_{dark}^{P}$ at $h\nu_{ph} \geq 2.3$ eV. More clearly this effect is demonstrated in the insert of Fig. 3c, where the dependence of the $n_{mob}^{P,mF}/n_{loc}^{P}$ ratio on the frequency of initiating photons is shown. Such dependences with more and less pronounced extremeness near characteristic photon energies $h\nu_{ph}$ = 1.89 and 2.86 eV were obtained for the $n_{mob}^{P,mF}/n_{loc}^{P}$ ratios of all samples under study. The analogous feature were registered in the study of low-bandgap copolymer OPV [41]. It was explained as a result of inhomogeneous distribution of high-energetic spin traps and different energy levels occupied by spins in these systems with specific morphology and band structure as well as a realization of some immobilized polarons out the spin traps under the action of photons of a corresponding energy. The results obtained evidence that interaction between spin ensembles governs the zone, molecular structures and effective electronic properties of such multispin composite. This effect can be used, e.g., for creation of light band-converters, optic filters and amplifiers.

Temperature dependences of the concentration ratio $n_{mob}^{P,mF}/n_{loc}^{P}$ determined for both charge carriers photoinitiated in the initial and optimally doped nanocomposites are shown in Fig. 4. The data presented evidence that the number of mobile polarons and methanofullerene radical anions decrease exponentially with the temperature growth, however, demonstrating an extreme temperature dependence with a characteristic point at $T \approx 107$ K. The analogous dependence was obtained for spin susceptibility of some poly(3-alkylthiophene):C_{60} polymer composites characterizing with the ferromagnetic↔antiferromagnetic balance [42] and low-bandgap copolymer:methanofullerene system [34]. Such effect was shown to be realized in some other multispin polymer systems [5a] due to an implementation of regimes of strong and weak spin coupling realizing at lower and higher temperatures, respectively [43]. This may mean the disbalance of these regimes upon the sample heating which realizes additional charge carriers localized in high-energetic spin traps.

According to the Miller-Abrahams tunneling model [44], the polaron diffusing between initial *i* and destinated *j* sites of a single polymer chain spends the difference of their energies ΔE_{ij}, In real

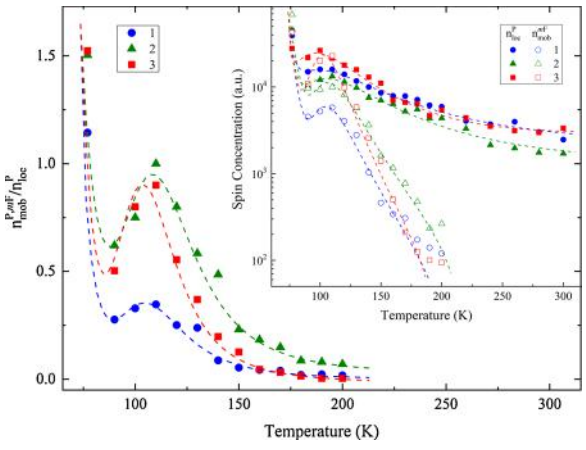

Fig. 4. Temperature dependences of concentrations (insert) as well as the respective concentration ratios $n_{mob}^{P,mF}/n_{loc}^{P}$ obtained for mobile methanofullerene radical anions $mF_{mob}^{-\bullet}$ and captured polarons $P_{loc}^{+\bullet}$ photoinitiated in the initial P3DDT:$PC_{61}BM$ BHJ (1) as well as in the P3DDT: $PC_{61}BM/BP_{0.03}$ (2) and P3DDT:$PC_{61}BM/PPO_{0.06}$ (3) samples. The dependences calculated from Eq. (1) with the energetic parameters summarized in Table 2 are shown by dashed lines.

polymer systems with closely spaced chains, it expectably interacts with the other spin packages that should also be taken into account [45,46]. The value of such interaction is determined mainly by the spin density on each polymer unit and the rate of spin intrachain diffusion with the expenditure of energy ΔE_{ij}. Generally, the relation for the effective paramagnetic susceptibility of polarons with spin $S = ½$ can be written as [43,47]

$$\chi(\Delta E_{ij}, E_a) = \chi_1 \exp\left(\frac{\Delta E_{ij}}{k_B T}\right) + \chi_2 \frac{2(1+\alpha^2)}{\alpha^2} \quad (1)$$

where χ_1 and χ_2 are constants, $\alpha = (3/2)J_{ex}/h\nu_{hop}$, J_{ex} is the amplitude of spin exchange during their collision and intrachain hopping diffusion with the rate $\nu_{hop} = \nu^0_{hop}\exp(-E_a/k_B T)$ and activation energy E_a, k_B is the Boltzmann constant, and h is the Plank constant. If the ratio J_{ex}/h is higher/less the frequency of spin collision, then the regime of strong/weak interaction is realized in the system. According to the spin exchange approach [45], the extremal character of resulting temperature dependency with characteristic temperature T_c should evidence the realization of both types of spin-spin interaction at $T \le T_c$ and $T \ge T_c$, respectively.

Temperature dependences calculated for the parameter $n^{P,mF}_{mob}/n^{P}_{loc}$ of charge carriers photoinitiated in the initial and optimally PPO- and DA-modified P3DDT:$PC_{61}BM$ composites under study are also shown in Fig. 4. It can be seen from the Figure that the data obtained experimentally for these samples are well approximated by the dependences calculated within the framework of the above approach from Eq. (1) with the energetic parameters summarized in Table 2. The value of amplitude of spin exchange J_{ex} lies near $J_{ex} = 0.110$ eV determined for P3DDT:$PC_{61}BM$ BHJ [43], and consistent with the energy typical for polaron formation in π-conjugated polymers, $E_p \approx 0.1$ eV [48].

3.3. Recombination of spin charge carriers

Fig. 5 shows how change effective LEPR spectra of the initial P3DDT:$PC_{61}BM$ and slightly doped P3DDT:$PC_{61}BM/PPO_{0.06}$ and P3DDT:$PC_{61}BM/DA_{0.03}$ composites excited at $h\nu_{ph} = 1.88$ eV and $T = 77$ K with the time after switching off the light. Decomposing these spectra becomes it possible to separate decay processes of mobile and captured spin charge carriers photoinitiated in these polymer matrices. The data presented evidence a significant decrease in the rate of recombination of mobile charge carriers in optimally doped samples originating their higher parameter n^{mF}_{mob}/n^{P}_{loc}. This fact may be interpreted in terms of sequential polaron hopping between spin traps formed in disordered polymer matrix. Localized polarons can either be retrapped by vacant trap site or recombine with opposite guest charge. Trapping and retrapping of a polaron reduces its energy that leads to its localization into energetically deeper trap and to the increase of number of localized polarons with the time. This process can be

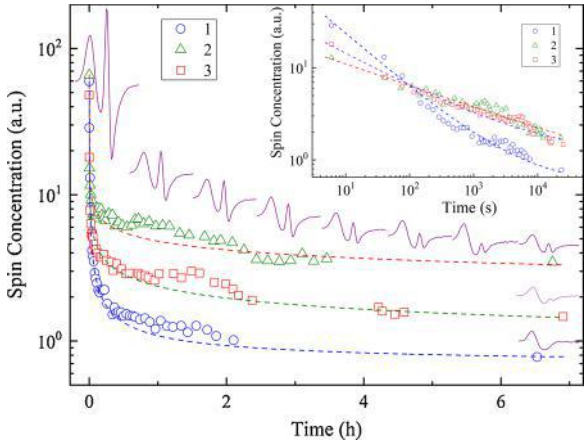

Fig. 5. The decay of the methanofullerene radical anions photoinitiated in the initial P3DDT: $PC_{61}BM$ (1), P3DDT:$PC_{61}BM/BP_{0.03}$ (2) and P3DDT:$PC_{61}BM/PPO_{0.06}$ (3) bulk heterojunctions by photons with $h\nu_{ph} = 1.88$ eV ($\lambda_{ph} = 660$ nm) at $T = 77$ K. Dashed lines show the dependences calculated from Eq. (2) well-fitting experimental data with E_0 summarized in Table 2.

described in terms of the Tachiya's approach [49] proposed for recombination of the charges during of their repeated trapping into and detrapping from trap sites with different energetical depth formed in disordered semiconductor. Such multiple trapping-detrapping model predicts the following law for decay of free charge carriers photoinitiated in polymer system with spin traps characterized by different energy depth [49]:

$$\frac{n(t)}{n_0} = \frac{\pi\alpha\delta(1+\alpha)\nu_d}{\sin(\pi\alpha)} t^{-\alpha} \quad (2)$$

where δ is the gamma function, $\alpha = k_B T/E_0$, ν_d is the attempt jump frequency for polaron detrapping, E_0 is distribution of energy depth of spin traps.

Fig. 5 shows that experimental data obtained for the initial P3DDT:$PC_{61}BM$ as well as slightly doped P3DDT:$PC_{61}BM/DA_{0.03}$ and P3DDT:$PC_{61}BM/PPO_{0.06}$ composites at $T = 77$ K can be described in terms of this approach implying E_0 summarized in Table 2. It is evident that the doping of the initial P3DDT:$PC_{61}BM$ composite by the DA and PPO molecules leads to the increase in the E_0 value that impedes recombination of mobile charge carriers. Therefore, the decay of long-lived charge carriers photoinduced in the polymer:fullerene bulk heterojunctions can indeed be described in terms of the above mentioned model in which the low-temperature recombination rate is strongly governed by the number and width of energy distribution of spin trap sites. This effect can be used to construct, e.g., organic devices accumulating electric energy.

Table 2
The energetic values of E_a, ΔE_{ij}, J_{ex} determined from Eq. (1), E_0 from Eq. (2), E_h from Eq. (3), E_b from Eq. (6), E_{es} from Eq. (7), E_{lr} from Eq. (8) for polarons $P^{+\bullet}$ and methanofullerene radical anions $mF^{-\bullet}$ photoinitiated in the initial P3DDT: $PC_{61}BM$, as well as in the P3DDT:$PC_{61}BM/BP_{0.03}$ and P3DDT:$PC_{61}BM/PPO_{0.06}$ composites.

Sample	P3DDT:$PC_{61}BM$			P3DDT:$PC_{61}BM/BP_{0.03}$			P3DDT:$PC_{61}BM/PPO_{0.06}$		
Carriers	$P^{+\bullet}$	$mF^{-\bullet}$	$mF^{-\bullet}$*	$P^{+\bullet}$	$mF^{-\bullet}$	$mF^{-\bullet}$*	$P^{+\bullet}$	$mF^{-\bullet}$	$mF^{-\bullet}$*
Parameter									
E_a, eV	0.1329	0.1278	0.0941	0.1527	0.1165	0.0667	0.1667	0.1288	0.0997
ΔE_{ij}, eV	0.0216	0.0555	0.0472	0.0257	0.0516	0.0531	0.0272	0.0650	0.0477
J_{ex}, eV	0.1235	0.2566	0.1458	0.3707	0.2277	0.1076	0.3548	0.2164	0.1103
$E_{0,}$ eV	–	0.0117	–	–	0.0173	–	–	0.0275	–
E_h, eV	0.0031	0.0009	–	0.0030	0.0012	–	0.0038	0.0008	–
E_b, eV	0.1033	–	–	0.0977	–	–	0.0855	–	–
E_{es}, eV	0.0293	–	–	0.0249	–	–	0.0285	–	–
E_{lr}, eV	–	0.4543	–	–	0.3462	–	–	0.2061	–

Notes: *Determined for the ratio $n^{P,mF}_{mob}/n^{P}_{loc}$.

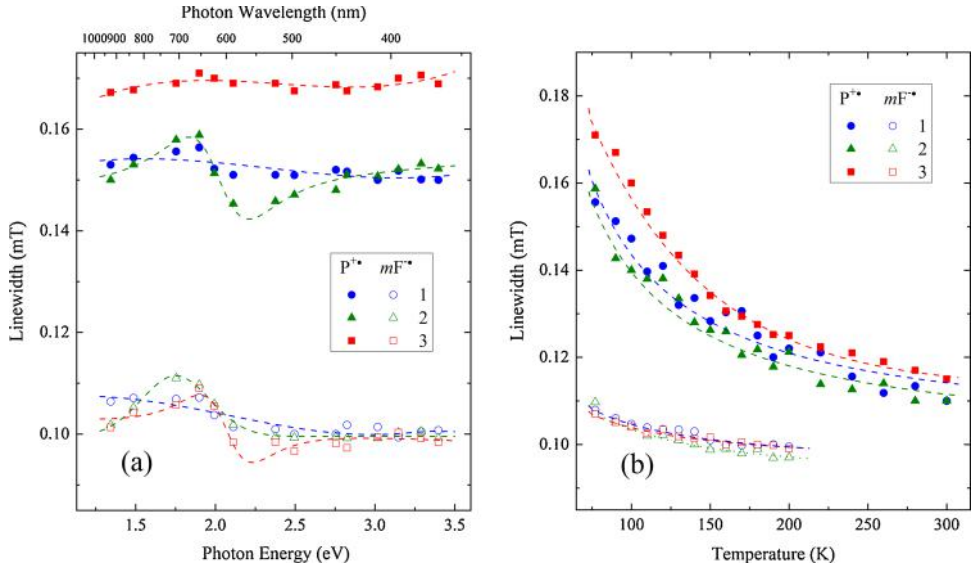

Fig. 6. Effective linewidth of polarons $O^{+\bullet}$ and methanofullerene radical anions l $E^{-\bullet}$, ΔB_{pp}^{P} and ΔB_{pp}^{mF}, respectively, photoinitiated in the P3DDT:$PC_{61}BM$ (1), P3DDT:$PC_{61}BM/BP_{0.03}$ (2) and P3DDT: $PC_{61}BM/PPO_{0.06}$ (3) composites as function of photon energy $h\nu_{ph}$ at T = 77 K (*a*) and temperature at $h\nu_{ph}$ = 1.88 eV (λ_{ph} = 660 nm) (*b*). The dashed lines in (*a*) are drawn arbitrarily only for illustration to guide the eye. The dashed lines in (*b*) show dependences calculated from Eq. (3) with respective E_h summarized in Table 2.

3.4. Linewidth of spin charge carriers

Fig. 6 shows how changes the peak-to-peak linewidth of polarons $P^{+\bullet}$, ΔB_{pp}^{P}, and methanofullerene radical anions $mF^{-\bullet}$, ΔB_{pp}^{mF}, in the P3DDT:$PC_{61}BM$, P3DDT:$PC_{61}BM/PPO_{0.06}$ and P3DDT:$PC_{61}BM/BP_{0.03}$ composites at variation of the energy of photons and temperature. It is seen from the data presented that this parameter of both charge carriers excited in the initial composite weakly depends on the energy of photons. This situation obviously changes upon its doping with the PPO and BP additives. The linewidth of polarons initiated in the P3DDT:$PC_{61}BM/PPO_{0.06}$ composite also demonstrate weak dependency on the photon energy. On the other hand, the ΔB_{pp}^{mF} value first increases with $h\nu_{ph}$ up to 1.85 eV, then decreases as the energy of photons reaches 2.2 eV and then returns to approximately its previous value at higher photon energy (Fig. 6a). One should to note that the value of positive extremum lies near that registered for the respective dependence of spin susceptibility mentioned above (see Fig. 3c). Meanwhile, such parameters obtained for the $P^{+\bullet}$ and $mF^{-\bullet}$ charge carriers excited in the P3DDT:$PC_{61}BM/BP_{0.03}$ composite were appeared to be changed nearly symbatically with the increase in photon frequency demonstrating maximum at 1.90 and 1.75 eV, respectively (Fig. 6a). This should to indicate a significant change in the morphology of the initial composite, originating an increase of the exchange interaction between their spin ensembles. Such interaction, however, seems to be weaker than in the case of other polymer multispin composites demonstrating more complex temperature dependences [5a,34,50]. The line of charge carriers should also be broadened due to interaction with the neighboring spins and lattice phonons. Fig. 6b exhibits temperature dependences of linewidths obtained for both the spin carriers transferring a charge in the P3DDT:$PC_{61}BM$, P3DDT:$PC_{61}BM/PPO_{0.06}$ and P3DDT:$PC_{61}BM/BP_{0.03}$ composites. Such dynamics can be described in terms of activation hopping of the carriers through a polymer backbone of composites and follow the following law:

$$\Delta B_{pp}(T) = \Delta B_{pp}^{hf} + \Delta B_{pp}^{0} \exp\left(\frac{E_h}{k_B T}\right), \quad (3)$$

where $\Delta B_{pp}^{hf} = 2/\sqrt{3}\gamma_e T_2$ is the linewidth of a single spin which randomly diffuses and hyperfine interacts with environmental nuclear spins of inhomogeneous polymer backbone, γ_e is the hyromagnetic ratio, T_2 is the spin-spin relaxation time, ΔB_{pp}^{0} is prefactor, and E_h is the energy required for the translational hopping of polarons in polymer backbone.

Fig. 6b shows the linewidths of both the charge carriers $P_{loc}^{+\bullet}$ and $mF_{mob}^{-\bullet}$ photoinitiated in polymer composites vs. temperature. As it is seen from the Figure, these values obtained for all BHJ follow well Eq. (3) with the E_h summarized in Table 2. The energetic parameters obtained evidence low interaction of these spins with own environment.

3.5. Spin relaxation and dynamics

LEPR spectrum shape also changes at its saturation regime which arises starting with a critical intensity of MW field at the location place of the sample. This allows to estimate spin-lattice T_1 and spin-spin T_2 relaxation times separately for both spin charge carriers in different polymer systems [5a,20] including P3DDT-based composites, e.g., [43,51]. These parameters provide information about the interaction of spin charge carriers with other paramagnetic centers and their environmental dipolar groups. Mobile spin carriers induce at their location an additional magnetic field whose strength is determined by their relaxation, number and dynamics. Because both the charge carriers possess different magnetic resonance parameters, it becomes to be possible to determine separately their translative and rotating dynamics parameters using the steady-state MW saturation method adopted for low-dimensional systems [32].

Fig. 7a depicts temperature dependences of spin-lattice, T_1^P and T_1^{mF}, and spin-spin, T_2^P and T_2^{mF}, relaxation times determined for polarons $P^{+\bullet}$ and methanofullerene radical anions $mF^{-\bullet}$, respectively, photoinitiated in the initial sample P3DDT:$PC_{61}BM$ as well as in the BP- and PPO-doped composites on the energy of initiating photons $h\nu_{ph}$. The data presented evidence a weak change of the $T_2(h\nu_{ph})$ values of both the charge carriers excited in all samples under study. On the other hand, their spin-lattice relaxation exhibits higher sensitivity to the photon energy. It is seen from the Figure that the T_1^P value of the polarons photoinitiated the initial sample changes extremely with the photon energy reaching a maximum at 1.90 eV. Its doping with the BP and PPO small molecules leads to the appearance in the dependences of the corresponding composites of the couple extrema located at 1.75, 2.72 eV and 1.70, 3.16 eV, respectively. At the same time, the spin-lattice relaxation of methonofullerene radical anions initiated in the initial and BP- and PPO-doped composites are characterized by the T_1^{mF} ($h\nu_{ph}$) dependences with characteristic points lying near 2.26 and

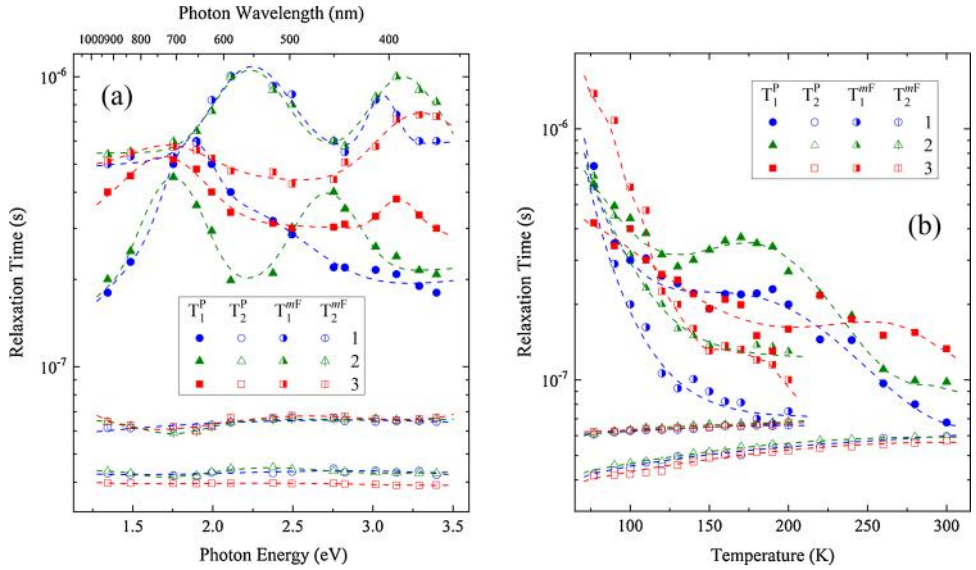

Fig. 7. Spin-Lattice and spin-spin relaxation times of mobile and captured polarons $O^{+\bullet}$, T_1^P (filled points) and T_2^P (open points), respectively, as well as methanofullerene radical anions $l\,E_{l\,na}^{-\bullet}$, T_1^{mF} (semi-filled points) and T_2^{mF} (open crossed points), respectively, photoinitiated in the P3DDT:$PC_{61}BM$ (1), P3DDT:$PC_{61}BM/BP_{0.03}$ (2) and P3DDT: $PC_{61}BM/PPO_{0.06}$ (3) composites as function of photon energy $h\nu_{ph}$ at $T = 77$ K (*a*) and temperature at $h\nu_{ph} = 1.88$ eV ($\lambda_{ph} = 660$ nm) (*b*). The dashed lines are drawn arbitrarily only for illustration to guide the eye.

3.06 eV, 2.23 and 3.19 eV, 1.74 and 3.32 eV (Fig. 7a). This effect can be associated with the π-π* transition of the samples with close optical bandgap and arises due to the changes in morphology, as well as in exchange interaction between different spin ensembles formed in polymer composites.

Fig. 7b shows the change in spin-spin and spin-lattice relaxation times of both the polarons $P^{+\bullet}$, and methanofullerene radical anions $mF_{mob}^{-\bullet}$ at the heating of the samples. As can be seen from the Figure, T_2 value of both charge carriers in all composites slightly monotonically increases with increasing temperature without any unusual features, which is typical for organic disordered semiconductors [20], including polymer:fullerene composites [5a]. Spin-lattice relaxation times of these charge carriers were expectable appeared to be more dependable on the temperature. This parameter of polarons decreases with the heating exponentially with different slope. As can be seen from the Figure, a well-pronounced bell-like contributions with characteristic point lying near 170 K appears in the dependences of the initial and BP-doped samples. This maximum is shifted to near 260 K as BP adduct is replaced by the PPO one (Fig. 7b). Such a change in the dependences' slope and shape can be explained by the above-mentioned difference in the structure and crystallinity of the initial and nanomodified samples that governs interchain spin interaction, polaron↔bipolaron balance or/and realizing of some polarons out of high-energetic spin traps upon their interaction with lattice phonons. Indeed, the bell-like contribution is absent in the T_1^{mF} (T) dependences which simply decrease exponentially with the temperature. Besides, the T_1^{mF} value increases at the doping of the initial P3DDT:$PC_{61}BM$ composite analogously to that occurring, e.g., in fullerene-modified poly({4,8-bis[(2-ethylhexyl)oxy] benzo[1,2-b:4,5-b']dithiophene-2,6-diyl}{3-fluoro-2-[(2-ethylhexyl) carbonyl]thieno[3,4-b]thiophenediyl}) (PTB7) with 1-pyrenebutyric acid butyl ester (PyBB) [9].

Polarons diffusing along and between the polymer chains with diffusion coefficients D_{1D}^P and D_{3D}^P, respectively, as well as rotational librations of methanofullerene globe near own main molecular axis with coefficient D_{lb}^{mF} induce additional magnetic fields that accelerates electron relaxation of whole spin ensemble. This allows to determine dynamics parameters of different spin ensembles from the relation connecting relaxation and dynamics parameters [52].

$$T_1^{-1}(\omega_e) = \langle\omega^2\rangle[2J(\omega_e) + 8J(2\omega_e)] \quad (4)$$

$$T_2^{-1}(\omega_e) = \langle\omega^2\rangle[3J(0) + 5J(\omega_e) + 2J(2\omega_e)] \quad (5)$$

where $\langle\omega^2\rangle = 1/10\ \gamma_e^4\hbar^2\ S(S+1)n\Sigma_{ij}$ is a constant of a dipole-dipole interaction in powder-like sample, n is a spin density in each backbone unit, Σ_{ij} is the lattice sum for powder-like sample, $J(\omega_e) = (2\ D_{1D}^{|}\ \omega_e)^{-1/2}$ (at $D_{1D}^{|} > > \omega_e > > D_{3D}^P$) and $J(\omega_e) = \tau_c/(1+\tau_c^2\omega_e^2)$ are spectral density functions for Q1D longitudinal and rotational libration spin hopping with correlation time τ_c, respectively [16,53], $D_{1D}^{|} = 4\ D_{1D}^P/L^2$, ω_e is angular resonant frequency of an electron spin precession, and L is a factor of spin delocalization along polaron equal to 4–5 monomer units in regioregular poly(3-alkylthiophenes) [54]. The value $L = 5$ was used for calculation of dynamics parameters of polarons in the initial and nanomodified composites under study.

Dynamics parameters calculated for both the charge carriers photoinitiated in the samples under study from Eq. (4) and (5) using the data presented in Fig.7 are shown in Fig. 8 as functions of the photon energy and temperature.

It is seen from the Fig. 8a that intrachain dynamics of polarons in the initial and BP-containing P3DDT:$PC_{61}BM$ composites is governed by the energy of initiated photons accelerating significantly around $h\nu_{ph} = 1.80$ eV. The same dependence obtained for PPO-modified sample is somewhat shifted to the higher energy band and demonstrates a similar tendency. The rate of polarons hopping between the chains of the initial BHJ first decreases with the increase of photon energy, reaches minimum at $h\nu_{ph} = 1.92$ eV and then continues to increase at higher photon energy. Such dependence becomes more complex upon its nanomodification (Fig. 8a). In the same time, the coefficient of libration dynamics of methanofullerene globes D_{lb}^{mF} was appeared to feel weaker the energetic of phonons. Because $D_{lb}^{mF} \propto 1/nT_1^{mF}$ (see Eq. (4)), this parameter may be affected by changes in concentration of radical anions due to recombination with the opposite polaron charges and interaction with other spin ensembles. The analogous conclusion may be made for the polaron intrachain hopping dynamics characterizing with the stronger relation $D_{1D}^P \propto (nLT_1^P)^2$.

Spin-assisted processes carrying out in the composites depend also on the spin charge carriers with the lattice phonons. Fig. 8b depicts the temperature dependences of dynamics parameters obtained for polarons, D_{1D}^P and D_{3D}^P, and methanofullerene radical anions, D_{lb}^{mF} photoinitiated by photons with $h\nu_{ph} = 1.88$ eV in the samples under study. The analysis of experimental data has shown that the intrachain charge dynamics can be described in terms of its activation hopping through

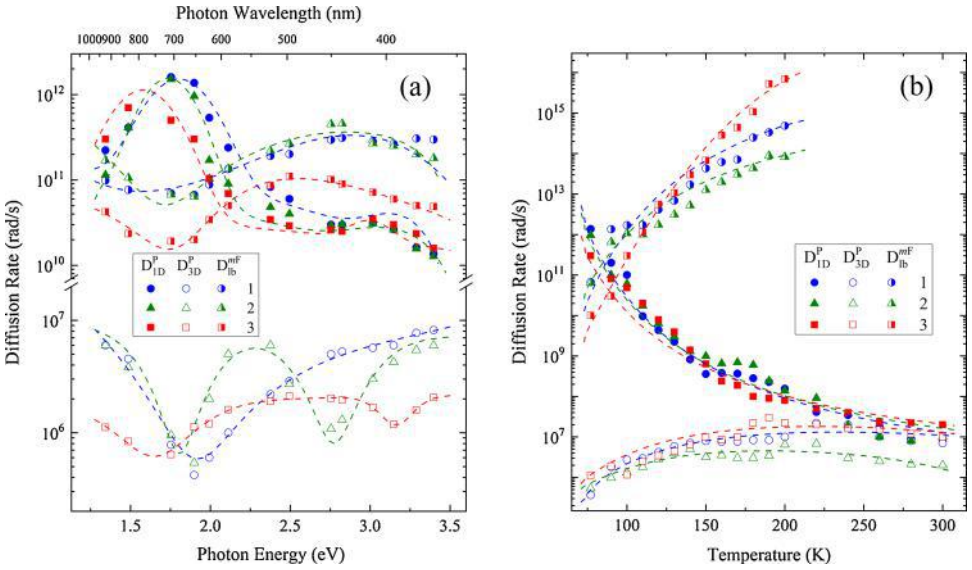

Fig. 8. Translational diffusion coefficients of intrachain, D^{P}_{1D} (filled points) and interchain (D^{P}_{3D}, open points) hopping of polarons $O^{+\bullet}$ as well as of libration rotational of methanofullerene radical anions $l\,E^{-\bullet}_{l\ na}$ (D^{mF}_{lb}, semi-filled points) photoinitiated in the P3DDT: $PC_{61}BM$ (1), P3DDT:$PC_{61}BM/BP_{0.03}$ (2) and P3DDT:$PC_{61}BM/PPO_{0.06}$ (3) composites as function of photon energy $h\nu_{ph}$ at T = 77 K (*a*) and temperature at $h\nu_{ph}$ = 1.88 eV (λ_{ph} = 660 nm) (*b*). The dashed lines in (*a*) are drawn arbitrarily only for illustration to guide the eye. The up-to-down series of dashed lines in (*b*) show dependences calculated from Eq. (6)–(8), respectively, with E_b, E_{es}, and E_{lr}, energies summarized in Table 2.

the energy barrier E_b [44].

$$D^{P}_{1D} = D^{0}_{1D}\exp\left(\frac{E_b}{k_B T}\right) \tag{6}$$

where D^{0}_{1D} is a constant. Charge hopping between the chains of polymer backbone seems more likely to be described within the framework of polaron activation hopping through respective BHJ [55],

$$D^{P}_{3D} = D^{0}_{3D} T^{2} \omega_e^{s} \exp\left(\frac{E_{es}}{k_B T}\right) \tag{7}$$

where $s = 1 - n_1 k_B T/E_{es}$, n_1 is a constant, and E_{es} is the energy for activation of charge carrier to the extended states. Finally, libration dynamics of methanofullerene radical anions can be described according the low

$$D^{mF}_{lb} = D^{0}_{lb}\exp\left(\frac{E_{lr}}{k_B T}\right) \tag{8}$$

where D^{0}_{lb} is a constant and E_{lr} is the energy required for initiation of libration dynamics of these charge carriers.

As follows from the Figure, the data obtained experimentally can be fitted well by the Eqs. (6) to (8) with respective energetic parameters summarized in Table 2, so then spin-dependent dynamics processes carrying out in the composite studied can, therefore, be described within the above approaches.

4. Conclusions

The effect of addition of the BP and PPO small molecules on spin-assisted initiation, relaxation, dynamics and recombination of charge carriers in organic photovoltaic blends formed by P3DDT as electron donor and $PC_{61}BM$ as electron acceptor was investigated by direct LEPR method. It was shown that the concentration, composition and dynamics of spin charge carriers are determined by the structure and morphology of P3DDT:$PC_{61}BM$ photovoltaic system as well as by the density and energy of the initiating light photons. The electronic and functional properties of such BHJ are governed by the number, spatial distribution and energy depth of spin traps formed in the polymer matrix due to its disordering. These properties were interpreted in the framework of exchange coupling of mobile and localized spins differently distributed in BHJ. Such interaction provokes higher overlapping of their wave functions which accelerates electron relaxation of all spin ensembles formed in the system under study. This eliminates the selectivity of the composite to the photon energy, controls the range of optical photons absorbed and, therefore, allows to create on their base a more efficient and functional electronic and spintronic elements. The results experimentally obtained showed that the stability and dynamics parameters of spin charge carriers photoinitiated in the BHJ become better after its optimal slight doping with BP and PPO molecules. At higher concentrations, these additives can form domains, which does not improve the functionality of the polymer composite. Such modification increases the number of free charge carriers due to the release of part of the localized carriers from energetically deep spin traps and an exchange interaction between these spin ensembles. Optimal number of the nanoadditives is less considerably than that of methanofullerene molecules in the initial OPV. This means that the nanoadditives used disenable somewhat improve the electronic properties of the whole acceptor phase in the system under study. They rather play role of a mediator of structuring/crystallization of the composite, analogously with the boiling of superheated (or crystallization of supercooled) liquids when adding some foreign nanoparticles. Such an effect may, probably, be additionally used in the novel fullerene-free molecular devices, in which small two-dimentional-molecules are used not only as electron acceptors but also as structural mediators. The method described can be used also to improve the electronic and functional characteristics of different donor-accepter systems.

Declaration of Competing Interest

The authors declare that they have no known competing financial interests or personal relationships that could have appeared to influence the work reported in this paper.

CRediT authorship contribution statement

V.I. Krinichnyi: Conceptualization, Project administration. **E.I. Yudanova:** Methodology, Investigation. **N.N. Denisov:** Investigation, Formal analysis. **V.R. Bogatyrenko:** Resources, Data curation.

Acknowledgments

This work was performed according the State Assignment, No. AAAA-A19-119032690060-9 with financial support from the Russian Foundation for Basic Research, Grant No. 18-29-20011-mk.

References

[1] W. Hu (Ed.), Organic Optoelectronics, Wiley-VCH Verlag, Weinheim, 2013.
[2] 2- ed., C. Brabec, U. Scherf, V. Dyakonov (Eds.), Organic Photovoltaics: Materials, Device Physics, and Manufacturing Technologies, vol. 1, Wiley-VCH, Weinheim, 2014.
[3] (a) S.-f. Wang, Y.-n. Liu, J. Yang, Y.-t. Tao, Y. Guo, X.-d. Cao, Z.-g. Zhang, Y.-f. Li, W. Huang, Chin. J. Polym. Sci. 35 (2017) 207–218;
(b) L. Meng, Y. Zhang, X. Wan, C. Li, X. Zhang, Y. Wang, X. Ke, Z. Xiao, L. Ding, R. Xia, H.-L. Yip, Y. Cao, Y. Chen, Science 361 (2018) 1094–1098.
[4] (a) K. Seki, K. Marumoto, M. Tachiya, Appl. Phys. Express 6 (2013) 051603;
(b) K. Seki, K. Marumoto, M. Tachiya, J. Appl. Phys. 53 (2014) 01AB13.
[5] (a) V.I. Krinichnyi, S. Thomas, D. Rouxel, D. Ponnamma (Eds.), Spectroscopy of Polymer Nanocomposites, 1 ed., Elsevier, Amsterdam, 2016, pp. 202–275 Ch. 9;
(b) M. Yabusaki, K. Marumoto, J. Photopolym. Sci. Technol. 31 (2018) 169–176;
(c) D. Xue, S. Kamiya, M. Saito, I. Osaka, K. Marumoto, ACS Appl. Energy Mater. 3 (2020) 2028–2036.
[6] G.I. Likhtenshtein, Electron Spin Interactions in Chemistry and Biology: Fundamentals, Methods, Reactions Mechanisms, Magnetic Phenomena, Structure Investigation, Springer, 2016.
[7] Y. Zhang, B.R. Gautam, T.P. Basel, D.J. Mascaro, Z.V. Vardeny, Synth. Met. 173 (2013) 2–9.
[8] A. Cominetti, A. Pellegrino, L. Longo, A. Tacca, R. Po, C. Carbonera, M. Salvalaggio, M. Baldrighi, S.V. Meille, Mater. Chem. Phys. 159 (2015) 46–55.
[9] C. Carati, N. Gasparini, S. Righi, F. Tinti, V. Fattori, A. Savoini, A. Cominetti, R. Po, L. Bonoldi, N. Camaioni, J. Phys. Chem. C 120 (2016) 6909–6919.
[10] H. Zhang, Y. Liu, B. Xu, G. Chen, C. Wang, S. Wen, Y. Li, L. Liu, W. Tian, Org. Electron. 67 (2019) 50–56.
[11] (a) M. Schadt, H. Seiberle, A. Schuster, Nature 381 (1996) 212–215;
(b) H.-J. Meyer, T. Wolff, Chem. Eur. J. 6 (2000) 2809–2817;
(c) R. Jakubiak, T.J. Bunning, R.A. Vaia, L.V. Natarajan, V.P. Tondiglia, Adv. Mater. 15 (2003) 241–244;
(d) C.K.M. Chan, C.-H. Tao, H.-L. Tam, N. Zhu, V.W.-W. Yam, K.-W. Cheah, Inorg. Chem. 48 (2009) 2855–2864;
(e) W. Jivaramonaikul, P. Rashatasakhon, S. Wanichwecharungruang, Photochem. Photobiol. Sci. 9 (2010) 1120–1125;
(f) G. Ambrosi, M. Formica, V. Fusi, L. Giorgi, E. Macedi, M. Micheloni, P. Paoli, R. Pontellini, P. Rossi, Inorg. Chem. 49 (2010) 9940–9948.
[12] (a) J.M. Lupton, D.R. McCamey, C. Boehme, ChemPhysChem 11 (2010) 3040–3058;
(b) K. Yonezawa, M. Ito, H. Kamioka, T. Yasuda, L.Y. Han, Y. Moritomo, Appl. Phys. Express 4 (2011) 122601/01–122601/03.
[13] G.R. Eaton, S.S. Eaton, Multifrequency electron paramagnetic resonance, in: S.K. Misra (Ed.), Theory and Applications, Wiley-VCH, Weinheim, 2011, pp. 719–754 Ch. 17.
[14] D. Davidov, F. Moraes, A.J. Heeger, F. Wudl, H. Kim, L.R. Dalton, Solid State Commun. 53 (1985) 497–500.
[15] K. Mizoguchi, J. Appl. Phys. 1 (34) (1995) 1–19.
[16] K. Mizoguchi, S. Kuroda, H.S. Nalwa (Ed.), Handbook of Organic Conductive Molecules and Polymers, vol. 3, John Wiley & Sons, Chichester, New York, 1997, pp. 251–317 Ch. 6.
[17] (a) M.N. Uvarov, L.V. Kulik, Appl. Magn. Reson. 44 (2013) 97–106;
(b) F. Kraffert, R. Steyrleuthner, S. Albrecht, D. Neher, M.C. Scharber, R. Bittl, J. Behrends, J. Phys. Chem. C 118 (2014) 28482–28493.
[18] S.K. Misra (Ed.), Multifrequency Electron Paramagnetic Resonance. Theory and Applications, Wiley-VCH, Weinheim, 2011.
[19] K.-u.-R. Naveed, L. Wang, H. Yu, R.S. Ullah, M. Haroon, S. Fahad, J. Li, T. Elshaarani, R.U. Khan, A. Nazir, Pol. Chem. 9 (2018) 3306–3335.
[20] V.I. Krinichnyi, Synth. Met. 108 (2000) 173–222.
[21] (a) S. Sensfuss, A. Konkin, H.K. Roth, M. Al-Ibrahim, U. Zhokhavets, G. Gobsch, V.I. Krinichnyi, G.A. Nazmutdinova, E. Klemm, Synth. Met. 137 (2003) 1433–1434;
(b) K. Marumoto, Y. Muramatsu, S. Kuroda, Appl. Phys. Lett. 84 (2004) 1317–1319.
[22] (a) A. Konkin, A. Popov, U. Ritter, S. Orlinskii, G. Mamin, A. Aganov, A.A. Konkin, P. Scharff, J. Phys. Chem. C 120 (2016) 28905–28911;
(b) A. Konkin, U. Ritter, A.A. Konkin, G. Mamin, S. Orlinskii, M. Gafurov, A. Aganov, V. Klochkov, R. Lohwasser, M. Thelakkat, H. Hoppe, P. Scharff, J. Phys. Chem. C 122 (2018) 22829–22837.
[23] J. Niklas, O.G. Poluektov, Adv. Energy Mater. 7 (2017) 1602226/01–1602226/28.
[24] S. Sensfuss, M. Al-Ibrahim, S.S. Sun, N.S. Sariciftci (Eds.), Organic Photovoltaics: Mechanisms, Materials, and Devices (Optical Engineering), CRC Press, Boca Raton, 2005, pp. 529–557.
[25] K. Tashiro, K. Ono, Y. Minagawa, M. Kobayashi, T. Kawai, K. Yoshino, J. Polym. Sci. B 29 (1991) 1223–1233.
[26] S. Sensfuss, M. Al-Ibrahim, A. Konkin, G. Nazmutdinova, U. Zhokhavets, G. Gobsch, D.A.M. Egbe, E. Klemm, H.K. Roth, Z.H. Kafafi, P.A. Lane (Eds.), Organic Photovoltaics IV, vol. 5215, SPIE, Bellingham, 2004, pp. 129–140.
[27] I. Novak, B. Kovač, J. Electron. Spectrosc. Relat. Phenom. 113 (2000) 9–13.
[28] D.L. Silva, L. De Boni, D.S. Correa, S.C.S. Costa, A.A. Hidalgo, S.C. Zilio, S. Canuto, C.R. Mendonca, Opt. Mater. 34 (2012) 1013–1018.
[29] S. Stoll, A. Schweiger, J. Magn. Reson. 178 (2006) 42–55.
[30] (a) O.G. Poluektov, S. Filippone, N. Martín, A. Sperlich, C. Deibel, V. Dyakonov, J. Phys. Chem. B 114 (2010) 14426–14429;
(b) J. Niklas, K.L. Mardis, B.P. Banks, G.M. Grooms, A. Sperlich, V. Dyakonov, S. Beaupré, M. Leclerc, T. Xu, L. Yue, O.G. Poluektov, Phys. Chem. Chem. Phys. 15 (2013) 9562–9574.
[31] J. Krzystek, A. Sienkiewicz, L. Pardi, L.C. Brunel, J. Magn. Reson. 125 (1997) 207–211.
[32] K. Marumoto, N. Takeuchi, T. Ozaki, S. Kuroda, Synth. Met. 129 (2002) 239–247.
[33] (a) V. Dyakonov, G. Zoriniants, M. Scharber, C.J. Brabec, R.A.J. Janssen, J.C. Hummelen, N.S. Sariciftci, Phys. Rev. B 59 (1999) 8019–8025;
(b) A.A. Baleg, M. Masikini, S.V. John, A.R. Williams, N. Jahed, P. Baker, E. Iwuoha, M.J. Mazumder, H. Sheardown, A. Al-Ahmed (Eds.), Functional Polymers, Springer, Cham, 2019, pp. 1–54 Ch. 3.
[34] V.I. Krinichnyi, E.I. Yudanova, N.N. Denisov, V.R. Bogatyrenko, J. Phys. Chem. C 123 (2019) 16533–16545.
[35] (a) J.P. Hare, H.W. Kroto, R. Taylor, Chem. Phys. Lett. 177 (1991) 394–398;
(b) J.H. Huang, C.P. Lee, Z.Y. Ho, D. Kekuda, C.W. Chu, K.C. Ho, Sol. Energy Mater. Sol. Cells 94 (2010) 22–28.
[36] (a) R.H. Goodwin, B.M. Pollock, Arch. Biochem. Biophys. 49 (1954) 1–6;
(b) D. Montanaro, R. Lavecchia, E. Petrucci, A. Zuorro, Chem. Eng. J. 323 (2017) 512–519.
[37] R. Luchowski, Chem. Phys. Lett. 501 (2011) 572–574.
[38] J.Z. Niu, G. Cheng, Z.H. Li, H.Z. Wang, S.Y. Lou, Z.L. Du, L.S. Li, Colloid Surf. A 330 (2008) 62–66.
[39] (a) M. Al-Ibrahim, H.K. Roth, M. Schroedner, A. Konkin, U. Zhokhavets, G. Gobsch, P. Scharff, S. Sensfuss, Org. Electron. 6 (2005) 65–77;
(b) C.K. Shin, H. Lee, Synth. Met. 140 (2004) 177–181.
[40] K. Harigaya, S. Abe, Phys. Rev. B 49 (1994) 16746–16752.
[41] (a) V.I. Krinichnyi, E.I. Yudanova, V.R. Bogatyrenko, J. Phys. Chem. Solids 111 (2017) 153–159;
(b) V.I. Krinichnyi, E.I. Yudanova, V.R. Bogatyrenko, Sol. Energy Mater. Sol. Cells 174 (2018) 333–341;
(c) V.I. Krinichnyi, E.I. Yudanova, V.R. Bogatyrenko, J. Photochem. Photobiol. A: Chem. 372 (2019) 288–295.
[42] T. Kawai, S. Okazaki, H. Mizobuchi, H. Araki, K. Yoshino, Synth. Met. 86 (1997) 2333–2334.
[43] V.I. Krinichnyi, E.I. Yudanova, N.G. Spitsina, J. Phys. Chem. C 114 (2010) 16756–16766.
[44] J. Nelson, Phys. Rev. B 67 (2003) 155209/01–155209/10.
[45] Y.N. Molin, K.M. Salikhov, K.I. Zamaraev, Spin Exchange: Principles and Applications in Chemistry and Biology, Springer-Verlag, Berlin Heidelberg, 1980.
[46] E. Houze, M. Nechtschein, Phys. Rev. B 53 (1996) 14309–14318.
[47] V.I. Krinichnyi, Appl. Phys. Rev. 1 (2014) 021305/01–021305/40.
[48] L. Zuppiroli, S. Paschen, M.N. Bussac, Synth. Met. 69 (1995) 621–624.
[49] M. Tachiya, K. Seki, Phys. Rev. B 82 (2010) 085201/01–085201/08..
[50] V.I. Krinichnyi, E.I. Yudanova, N.N. Denisov, J. Chem. Phys. 141 (2014) 044906/01–044906/11.
[51] V.I. Krinichnyi, Sol. Energy Mater. Sol. Cells 92 (2008) 942–948.
[52] F. Carrington, A.D. McLachlan, Introduction to Magnetic Resonance With Application to Chemistry and Chemical Physics, Harrer & Row, Publishers, New York, Evanston, London, 1967.
[53] M. Nechtschein, T.A. Skotheim, R.L. Elsenbaumer, J.R. Reynolds (Eds.), Handbook of Conducting Polymers, Marcel Dekker, New York, 1997, pp. 141–163 Ch. 5.
[54] (a) F. Devreux, F. Genoud, M. Nechtschein, B. Villeret, H. Kuzmany, M. Mehring, S. Roth (Eds.), Electronic Properties of Conjugated Polymers, vol. 76, Springer-Verlag, Berlin, 1987, pp. 270–276;
(b) M. Westerling, R. Osterbacka, H. Stubb, Phys. Rev. B 66 (2002) 165220/01–165220/07.
[55] (a) M. El Kadiri, J.P. Parneix, H. Kuzmany, M. Mehring, S. Roth (Eds.), Electronic Properties of Polymers and Related Compounds, vol. 63, Springer-Verlag, Berlin, 1985, pp. 183–186;
(b) P. Jayakrishnan, M.T. Ramesan, Polym. Compos. 39 (2018) 2791–2800.